

LOW-LEVEL WINDS IN TORNADOES AND POTENTIAL CATASTROPHIC TORNADO IMPACTS IN URBAN AREAS

BY JOSHUA WURMAN, CURTIS ALEXANDER, PAUL ROBINSON, AND YVETTE RICHARDSON

A large and/or violent tornado crossing a densely populated area such as Chicago could cause widespread damage and mortality—with thousands of deaths in some modeled scenarios.

RADAR OBSERVATIONS OF INTENSE TORNADOES. Tornadoes are among the most intense and destructive atmospheric phenomena. Winds can exceed 100 m s^{-1} over limited areas causing nearly total destruction of structures and loss of life (Wurman et al. 1996; Wurman and Gill 2000; Wurman 2002; Alexander and Wurman 2005; Marshall 2004). In the United States over 1,000 tornadoes occur annually (Grazulis 1993), but they are difficult to predict, and average warning lead times are only 10–15 minutes, meaning that, unlike with hurricanes, many people are unable to leave

their homes in the tornado paths (Simmons and Sutter 2005). Fortunately, tornadoes usually spend most or all of their lifetimes over sparsely populated areas. In addition, only a small fraction of tornadoes (1%–10%) are capable of causing the most intense damage. Despite over 1,000 tornadoes annually, tornado deaths in the United States are relatively rare, averaging 60 per year (Grazulis 1993). Unfortunately, on the rare occasions when intense tornadoes cross populated areas, widespread damage can occur (Grazulis 1993; Brooks and Doswell 2001; Speheger et al. 2002; Doswell et al. 2006; Forbes 2006). The worst historical tornadoes in terms of deaths were the Tri-State tornado of 18 March 1925, causing 695 deaths, and the Natchez, Mississippi, tornado of 7 May 1840, causing 317 deaths. Damage caused by individual tornadoes to structures has exceeded \$1,000,000,000 (Brooks and Doswell 2001).

The areal extent of cities and surrounding densely populated suburbs is growing and it is inevitable that someday a large, intense, and long-track tornado will impact a densely populated urban or suburban region. To quantify accurately the potential consequences of a violent tornado crossing an urban area, it is necessary to know the precise distribution of winds in the most intense tornadoes. However, in nearly all tornadoes

AFFILIATIONS: WURMAN AND ROBINSON—Center for Severe Weather Research, Boulder, Colorado; ALEXANDER—University of Oklahoma, Norman, Oklahoma; RICHARDSON—The Pennsylvania State University, University Park, Pennsylvania

CORRESPONDING AUTHOR: Joshua Wurman, Center for Severe Weather Research, 1945 Vassar Circle, Boulder, CO 80305
E-mail: jwurman@cswr.org

The abstract for this article can be found in this issue, following the table of contents.

DOI:10.1175/BAMS-88-1-31

In final form 31 July 2006
©2007 American Meteorological Society

the actual intensity, radius of maximum winds, rate of decrease of winds away from the tornado core, and other structural metrics are unknown except in the most qualitative sense. Intensity is inferred only well after the tornado's passage from the actual damage that occurs using the Fujita scale and its recent enhancements (Marshall 2004; Letzmann 1923; Fujita 1971, 1992). The intensity of strong tornadoes as they cross over areas devoid of engineered structures and vegetation cannot be determined ac-

curately using these methods (Doswell and Burgess 1988). The resulting maps of actual damage (Spehger et al. 2002) inevitably underestimate the maximum damage potential of these tornadoes. Previously, efforts have been made to estimate the effect of hypothetical tornadoes crossing urban areas (Rae and Stefkovich 2000; information online at www.nctcog.org/weather/study/), but these have been conducted by superimposing damage tracks from a tornado (the 3 May 1999 Bridgecreek–Moore, Oklahoma, tornado)

that passed over largely rural terrain onto a different urban area (Dallas–Fort Worth, Texas). Since the portions of the actual damage track that were over rural regions in Oklahoma likely underestimated the full damage potential of the tornado, the resultant transposition also likely underestimated significantly the potential for damage if that same tornado had crossed through extensive lengths of high-density single-family housing.

The Doppler-on-Wheels (DOW; Wurman et al. 1997; Wurman 2001) network of mobile Doppler weather radars has observed over 100 different tornadoes at various elevations, producing two- and three-dimensional high-resolution wind fields, typically at 30–60-s intervals, permitting relatively precise characterization of the structure, intensity, and evolution of the tornadoes (Wurman et al. 1996; Wurman and Gill 2000; Alexander and Wurman 2005; Burgess et al. 2002; Wurman et al. 2007a,b). Tornado observations from other mobile radars have also been produced (Bluestein and Pazmany 2000; Bluestein et al. 2003, 2004). In rare cases, these wind fields

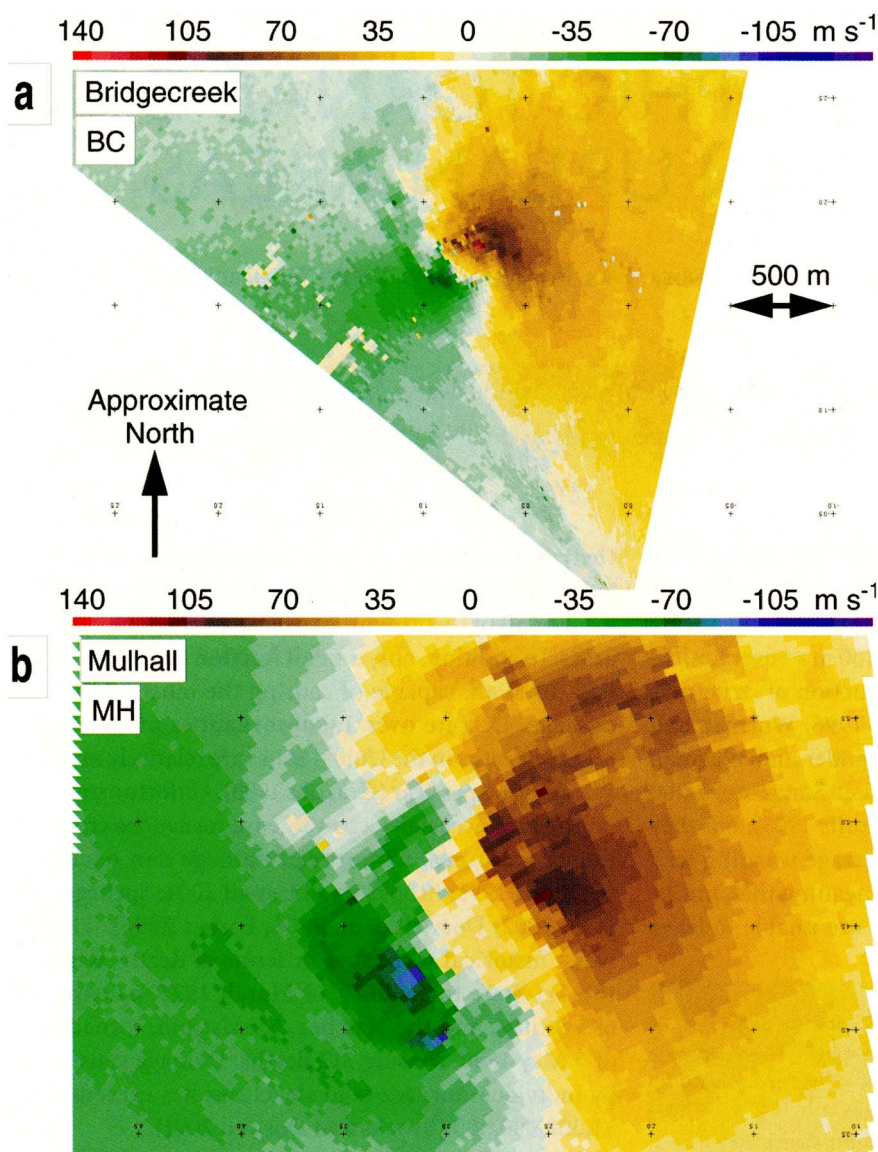


FIG. 1. DOW-measured Doppler velocity in two intense tornadoes. Couplets of positive (brown/red) and negative (green/blue) Doppler velocities denote tornadic winds. (a) Bridgecreek, OK, at 2354 UTC 3 May 1999. Peak ground relative winds of 135 m s^{-1} occur at 32 m AGL at a range of 1.9 km in a roughly 350-m diameter circulation. (b) Near Mulhall, OK, at 0313 UTC 4 May 1999. Peak winds over 105 m s^{-1} are observed at this time and 115 m s^{-1} were observed at other times in a circulation with diameter 1100 m at this time and up to 1600 m at other times at 30 m AGL at a range of 4–5 km.

have been compared to actual surveyed damage (Wurman and Alexander 2005). While most tornadoes are relatively weak, DOWs have measured winds in several intense tornadoes, with Doppler winds in the strongest exceeding 100 m s^{-1} below 50 m AGL.

Based on DOW Doppler data, peak Doppler wind speeds of 135 m s^{-1} occurred at 32 m AGL in a tornado crossing Bridgecreek, Oklahoma, at 2354 UTC 3 May 1999 (Fig. 1), the strongest ever measured in a tornado (Glenday 2006). There is F5 intensity (Fujita 1971) damage, consistent with these wind speeds, documented in the Bridgecreek development near the location of this measurement (Speheger et al. 2002), and later, 25 km distant, in Moore, Oklahoma, caused by the same tornado.

The DOW3 radar operates at a frequency of 9.375 GHz with a beam width of 0.93° . A staggered pulse repetition frequency scheme (Doviak and Zrnica 1993) is used to produce a Nyquist unambiguous velocity range of 256 m s^{-1} (from $+128$ to -128 m s^{-1}). Data where normalized coherent power is < 0.2 or where values exceed the median of nearest neighbors by 0.4 times the Nyquist value are eliminated. This eliminates outlier Doppler velocities that range as high as 142 m s^{-1} . Data are dealiased in the rare cases where Doppler velocities exceed 128 m s^{-1} . The Bridgecreek–Moore (hereinafter BC) tornado was moving at a 29° angle at 9.0 m s^{-1} relative to the DOW radar beams, necessitating adjustment of the maximum Doppler velocities, which were 134.0 m s^{-1} , by 1.0 m s^{-1} , resulting in a peak ground-relative wind velocity of 135.0 m s^{-1} (i.e., relative to a stationary observer). Several measurements exceeding 110 m s^{-1} are adjacent to the highest Doppler value, as required by the filtering described above, and lend credibility to the measurement. Estimated spectral widths were $15\text{--}20 \text{ m s}^{-1}$ in the most intense region of the tornado, suggesting that the measured Doppler velocities are likely only accurate within $\pm 5 \text{ m s}^{-1}$, so the resultant ground relative velocity is $135 \pm 5 \text{ m s}^{-1}$. These wind speeds were measured in a region extending across about 100 m. Air parcel trajectories could not be

calculated, but it is likely that wind speeds averaged over 3 s were several meters per second lower. Doppler measurements represent mean wind speeds inside a radar resolution volume. It is certain that short-duration and small-scale wind gusts higher than the means are present. As discussed later, care must be taken when comparing these Doppler measurements at 32 m AGL to time-averaged anemometer measurements at 3 or 10 m or inferences from damage occurring at 3–5 m AGL.

The region containing the maximum intensity winds of the BC tornado is measured by the DOWs to have a diameter of 350 m, which is above average for DOW-observed tornadoes, but is not the largest (Table 1). Other intense tornadoes have had much larger core flows, resulting in much broader regions of extreme winds. The largest tornadic core flow region ever measured by the DOWs, or in fact ever documented (Glenday 2006), occurred later during the same tornado outbreak, at 0310 UTC 4 May 1999 near the town of Mulhall, Oklahoma. While the peak winds measured by the DOW at 30 m AGL in the Mulhall (hereinafter MH) tornado are only $110\text{--}115 \text{ m s}^{-1}$, the diameter of the core flow region is as large as 1600 m at some observation times. Wind speeds capable of causing significant damage, $> 43 \text{ m s}^{-1}$, extended across a swath over 7 km wide (Table 1), which is substantially wider than the damage swath of the Hallam, Nebraska, tornado of 22 May 2004 (McCarthy and Schaefer 2005). As with the Doppler measurements over Bridgecreek, care must be exercised when comparing these measurements with wind estimates derived from damage or conventional anemometer measurements due to the differences in observation height, spatial and temporal averaging, and sampling.

The BC tornado destroyed more than 1,500 homes and killed 36 people. Despite this regrettable damage and resultant loss of life, it is fortunate that the BC tornado spent much of its lifetime over sparsely populated rural regions and did not cross over even more populated regions of the Oklahoma City metropolitan

TABLE 1. Tornado parameters and width (m; D_{xx}) of track $|V_h|$ greater than thresholds (m s^{-1}) indicated by “ D_{xx} .” HN, H2, H3, H4, H5, H6, H7: Same as HB.

Tornado	V_{rm}	R	b	g	V_t	D_{43}	D_{59}	D_{76}	D_{102}	D_{120}
MH Mulhall	100	700	-0.6	l	13	7050	3760	2355	757	—
BC Bridgecreek/Moore	126	175	-0.6	l	9	2315	1280	835	506	320
HB Hybrid	125	700	-0.6	l	7	8800	5050	3270	1985	1327
HR Hybrid reduced	105	700	-0.6	l	7	6580	3710	2450	1121	—
SM Small	75	100	-0.6	l	7	548	313	133	—	—

area, that Moore was near the end of the tornado track resulting in unusually long warning time to residents, and that the population densities in the Oklahoma City metropolitan area are low compared to those in other cities (Fig. 2). The MH tornado crossed almost entirely over rural low-population-density terrain containing few structures, so a wide damage swath was not documented.

In this paper, we examine the potential impacts if these or other large, violent, and/or long-track tornadoes crossed densely populated urban areas.

NEAR-SURFACE WINDS IN TORNADOES.

Radar temporal and spatial sampling and spatial averaging within radar resolution volumes preclude exact comparisons with surface-based anemometers that employ different sampling and temporal averaging, and measure at single points. In addition, radars measure scatterer motion, not air motion, resulting in possible underestimation of the latter in intense tornadoes (Dowell et al. 2005). The stan-

dard height for meteorological wind measurements (World Meteorological Organization 2004), and that now used to correlate wind speeds and damage to buildings (Marshall 2004), is 10 m AGL and is a 3-s average. Typical residential structures extend from 0 to 10 m AGL, while the DOW measurements of the BC and MH tornadoes are taken at about 30 m. Radar beam spreading by 16 m km^{-1} and blockage by foliage, buildings, and terrain usually preclude measurements by radar below 30 m AGL. On one occasion (8 June 1998), when a tornado center was at a range of 170 m and maximum winds were at a range of 30 m, a DOW observed winds near 10 m AGL. The observation is at a sufficiently low level to reveal axisymmetric convergence of 0.10 s^{-1} , evidenced by the slight rotation of the Doppler velocity couplet (Fig. 3). Axisymmetric convergence is estimated using $\nabla \cdot \mathbf{V} = 2(\Delta V / \Delta x) \cos(\alpha)$, where ΔV is the Doppler velocity difference across the couplet, Δx is the distance from the inbound to outbound Doppler velocity extrema, and α is the angle between the vectors drawn from the positive to the negative velocity extrema and the radar beam from the radar to the center of circulation. [A similar calculation, using $\sin(\alpha)$, where α is the angle between the radar beam through the center of the tornado and the zero isodop contour through the tornado, provides a consistent result.] The observed convergence is slightly higher than the value of 0.06 s^{-1} observed by Alexander and Wurman (2005) at a higher altitude in a much more intense tornado.

While having these low-level radar observations is useful, having a tornado core flow pass within 30 m of a DOW is not a desirable or frequently realized observational strategy. In order to evaluate how DOW wind measurements typically collected at altitudes above 30 m AGL should be corrected to the 10-m-AGL level, the dependence of peak winds with height in the lowest 200 m AGL is calculated in two tornadoes where particularly low-level DOW observations are available. The rotational velocity of tornadoes increases rapidly with decreasing altitude from 1000 m AGL down to 100 m AGL (Wurman and Gill 2000; Alexander and Wurman 2005). However, peak winds on the track-relative right-hand side of some tornadoes are observed by DOWs to be relatively constant from 20 to 200 m AGL (Fig. 4).

Below 20 m AGL, frictional effects due to the ground, structures, and foliage likely cause wind speeds to decrease, dropping of course to 0 m s^{-1} at the ground. In situ measurements of tornadoes are rare (Winn et al. 1999; Lee et al. 2004; Wurman and

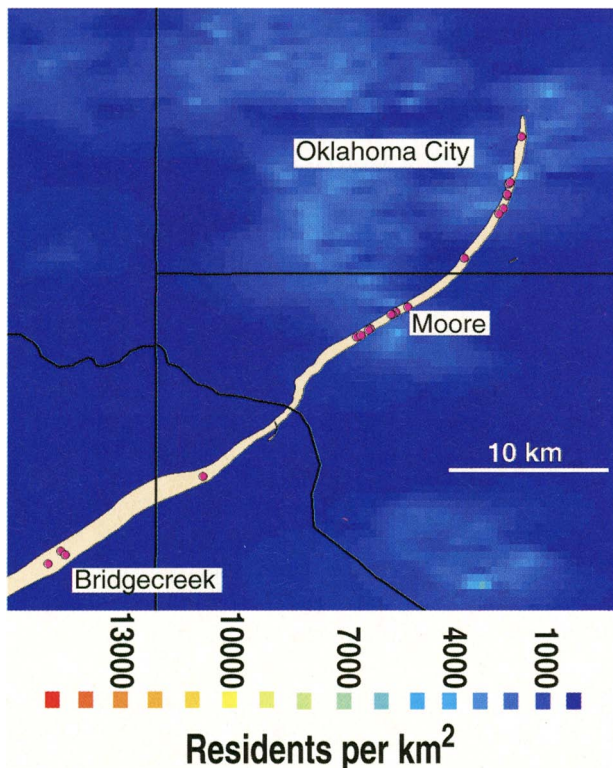


FIG. 2. Track of Bridgecreek-Moore tornado and population density. The track of the tornado crossed largely over rural and low-density suburban regions of central Oklahoma with population densities $< 4000 \text{ km}^{-2}$. Most fatalities (pink dots) were associated with brief crossings of populated low-medium-population-density suburban regions in Bridgecreek, Moore, and south-eastern Oklahoma City.

Samaras 2004) and do not usually produce wind speed data. In 2005, the first combined DOW radar and near-surface in situ wind measurements were obtained, permitting the evaluation of the dependence of tornado wind speeds on height below 20 m AGL. On 12 June 2005, near Jayton, Texas, a DOW measured Doppler winds at 18 m AGL above an armored instrumented vehicle at the edge of a tornado, while the center of the core flow passed 100 m to the east of the instrumented vehicle (Fig. 5). The instrumented vehicle measured wind speeds, $|\mathbf{V}|$, up to 38 m s^{-1} at 3 m AGL using a conventional mast-mounted ultrasonic anemometer (0.1-s sampling every 1 s). After correcting for DOW observation geometry relative to the tornado, specifically accounting for the difference in wind direction and the direction of the DOW radar beams, and interpolating between DOW observations that were spaced at 20-s intervals, the time history of winds at 18 and 3 m AGL can be compared (Fig. 6): $|\mathbf{V}_{3 \text{ m AGL}}|/|\mathbf{V}_{18 \text{ m AGL}}| = 0.74$ to 0.80 , though there are transient fluctuations, during the tornado's passage. This suggests that $|\mathbf{V}_{10 \text{ m AGL}}|/|\mathbf{V}_{18-150 \text{ m AGL}}| = 0.9$, approximately. (It matters little whether linear, log, or other interpolations are used since the scan-to-scan variation exceeds the differences in interpolation profiles.) The implied 10% reduction in winds from 18 to 10 m AGL is less than the sweep-to-sweep variability between 20 and 200 m AGL wind speeds evident in Fig. 4. These data suggest that DOW measurements at 30 m AGL may be reasonably representative of conditions at 10 m AGL, at least in some tornadoes, in some terrain conditions.

The 12 June 2005 observations occurred in a region devoid of tall trees and buildings (Fig. 7). It is likely that tornadic wind speeds at 10 m AGL are less when a substantial fraction of the ground surface is covered by structures, increasing the effective surface roughness. However, no observational data exist to quantify this effect in tornadoes. Wind speeds are likely 25% less close to the ground at the midlevel height of one- or two-story residential structures, as suggested by the 3-m-AGL in situ measurements. Additionally, the in situ measurements were obtained outside the core flow region of the tornado. The variation of peak

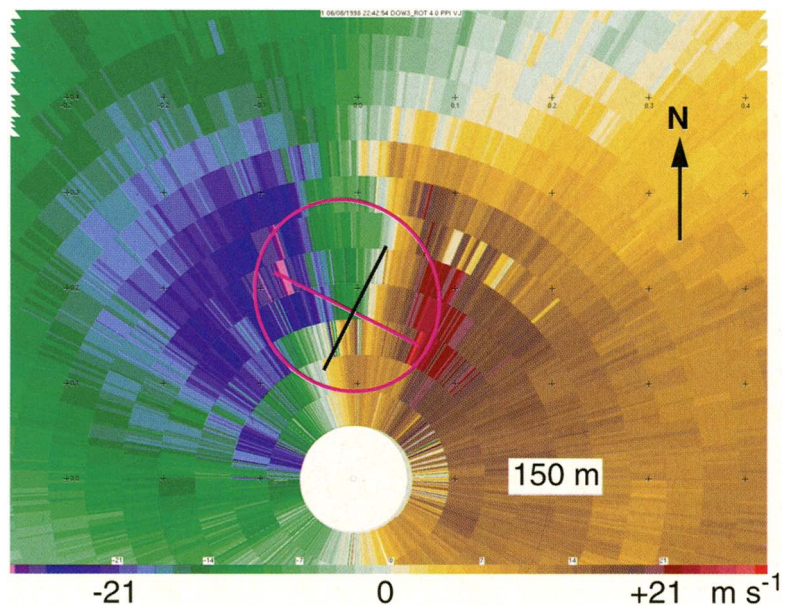


FIG. 3. Doppler velocity in a tornado passing a DOW at extremely close range. The tornado center passed within 170 m from a DOW, with the region containing maximum winds (pink circle) passing 30 m from the DOW. This close approach permitted measurements at an unusually low altitude near 10 m AGL. The data were collected near Cambridge, KS, on 8 Jun 1998. Convergence of 0.1 s^{-1} is revealed from the orientation of the line (pink) connecting the inbound and outbound wind maxima and the rotation of the zero isoDop line (black).

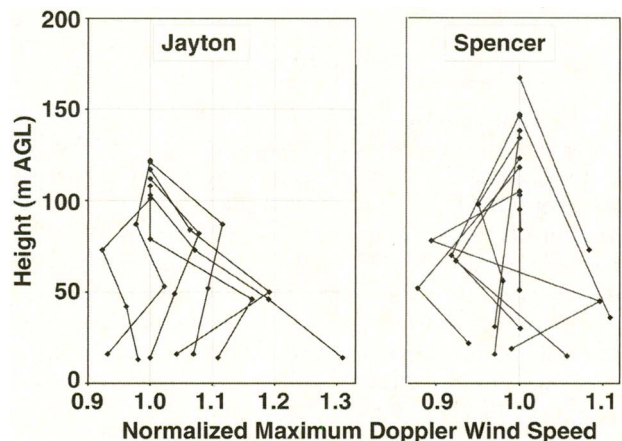


FIG. 4. Normalized peak Doppler wind velocities observed by DOWs in low levels of two tornadoes exhibit little dependence on altitude below 150 m AGL. (left) Jayton, TX, 12 Jun 2005. (right) Spencer, SD, 30 May 1998. Peak Doppler velocities measured at levels below 100 m AGL are normalized by the values observed at the level closest to and above 100 m. Measurements taken during individual 20-s periods are connected with lines. No clear dependence of velocity on height is apparent, though a slight increase at the lowest levels is suggested in the Jayton tornado. Measurements taken at 2350–2358 UTC at a range of 2–3 km from the Jayton tornado and from 2334–2340 UTC at a range of 1.7–5.0 km from the Spencer tornado.

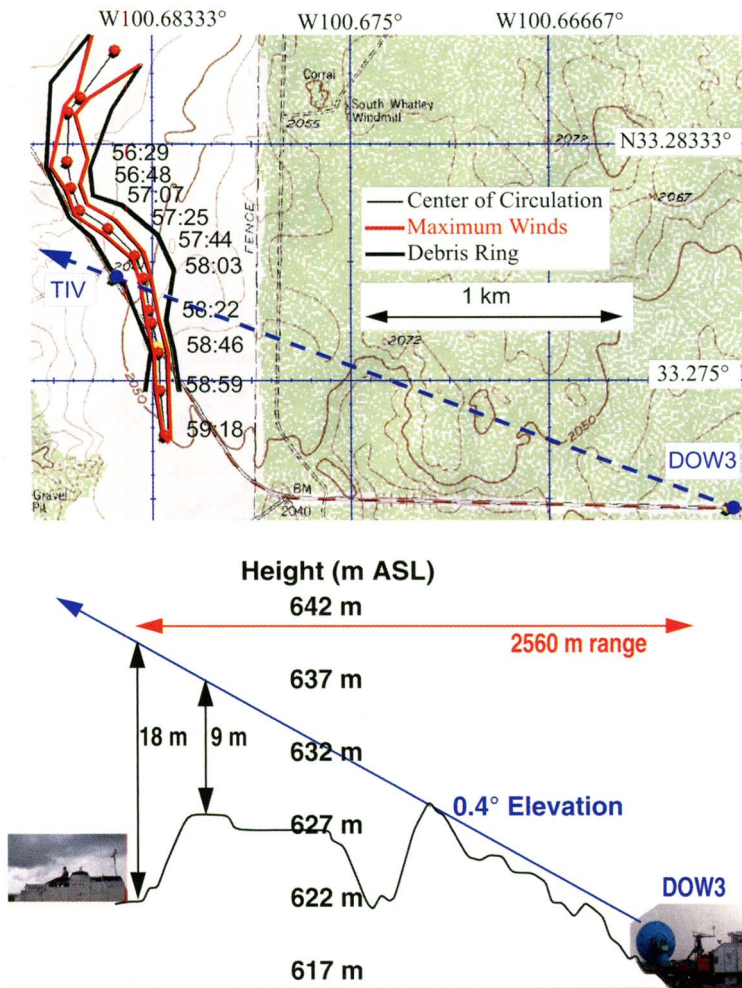


FIG. 5. Deployment of DOW and Tornado Intercept Vehicle (TIV) to measure low-level winds in a tornado near Jayton, TX. (top) The locations of the DOW and TIV and the path of the tornado. Times are MM:SS after 0000 UTC 13 Jun 2005. The center of circulation of the tornado passed 100 m to the east of the TIV. The small core flow region of the tornado missed the TIV, which was at the radius of the DOW-measured debris ring. (bottom) The TIV measured winds using an ultrasonic anemometer mounted at 3 m AGL (0.1-s samples every 1 s). Because of radar beam spreading and terrain blockage, the lowest-level winds measured by the DOW were at 18 m AGL over the TIV (which was in a slightly depressed area).

wind speed with height may be substantially different inside and outside the core flow region.

SIMULATIONS OF TORNADO WINDS BASED ON DOW DATA. As can be seen from Fig. 1, the wind field of actual tornadoes can be complex. Furthermore, single-Doppler radars can only measure the component of wind field parallel to the direction of radar beam propagation. In order to reconstruct the full horizontal wind field impinging on structures, an axisymmetric wind field model of a translating tornado, constrained by DOW observa-

tions (Wurman and Alexander 2005), is fit to profiles of radial velocity. Ground-relative horizontal wind speeds, $|V_h|$, are calculated (Fig. 8) by

$$|V_h| = [V_t^2 + V_r^2 + V_i^2 + 2(V_t)(V_i)\cos(a) + 2(V_r)(V_i)\sin(a)]^{1/2},$$

where V_t is the translational speed of the tornado vortex, V_r is the rotational velocity (positive is counterclockwise) of the vortex, V_i is the inflow velocity (positive is outward), and a is the angle between the direction of tornado motion and the location of the calculation,

$$V_r = V_{rm}(D/R)^\gamma \text{ when } D \leq R,$$

$$V_r = V_{rm}(R/D)^\beta \text{ when } D > R,$$

where R is the radius of maximum winds, γ and β are the decay rates of winds inside and outside the radius of maximum winds, and D is the horizontal distance from the center of the tornado. The values of V_t , V_{rm} , R , γ , and β are determined by DOW observations of the tornadoes to be simulated. The sign and radial profile of V_i depends on whether the tornado vortex exhibits single- or two-celled structure (Fiedler and Rotunno 1986; Lewellen et al. 1997). Observations of V_i in actual tornadoes vary (Wurman et al. 1996; Wurman and Gill 2000;

Alexander and Wurman 2005; Lee and Wurman 2005), and the conditions that result in the differing structures are not known; therefore, V_i is set to 0 m s^{-1} in these tornado simulations.

Different tornadoes may have substantially different wind field structures (e.g., Wurman and Gill 2000 versus Wurman 2002), and both the horizontal and vertical distribution of winds may differ markedly from tornado to tornado. The structure assumed in this model is merely representative of a simplified tornado. Simulated winds are calculated at 10-m intervals and a profile of maximum winds is

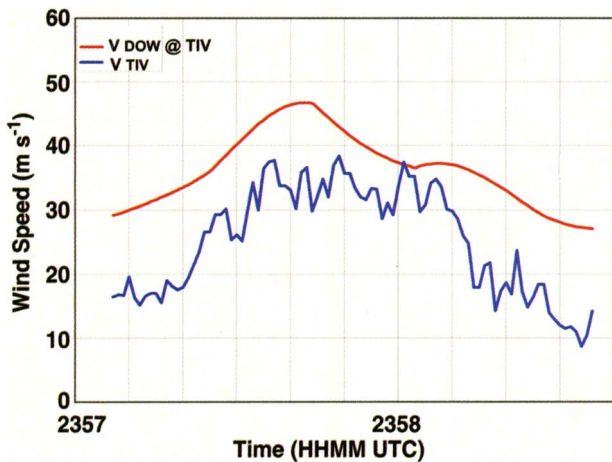


FIG. 6. Time history of ground-relative winds at 18 m AGL as calculated using DOW data, and measured 3-m winds as measured by TIV. The TIV data, recorded every second, indicate that $|V_h|$ at 3 m AGL is about 74% to 80% of that at 18 m AGL.

generated. This profile is slid across the various urban domains. Due to the slowly varying simplified wind field (about 10 m s^{-1} translation and tornado core flow diameters of 200–1400 m), the calculated peak wind speeds at individual points closely correspond to peak 3-s duration gusts, consistent with engineering and damage intensity estimation standards.

Impact of different tornadoes with same track. Using this observation-constrained model, the spatial distribution of peak winds, $|V_h|$, experienced by structures can be calculated for many possible real and hypothetical tornado scenarios, varying in intensity, size, translational velocity, and location. The physical properties of several tornadoes, including the width of the swaths containing $|V_h|$ in excess of the listed thresholds, are in Table 1.

The parameters of tornadoes MH and BC represent those observed in the actual tornadoes at their maximum DOW-observed intensity. The tornadoes might have been even more intense during the periods when they were not observed by DOWs. Dowell et al. (2005) suggest that the effects of debris centrifuging result in the underestimation of tornado winds by radars such as

the DOWs, particularly in small, intense tornadoes such as BC. A hypothetical “hybrid” tornado’s (HB) parameters represent the large size of the MH tornado and the peak intensity of the BC tornado. A slow tornado translational motion of 7 m s^{-1} , typical of many tornadoes (Wurman et al. 1996; Wurman and Gill 2000; Phan and Simiu 1998), is chosen to minimize the asymmetry between winds on the right and left sides of the HB tornado track. Slow translational speeds affect the duration of intense winds over individual locations (Wurman and Alexander 2005; Phan and Simiu 1998), which might have a very significant impact on resulting damage (e.g., the Jarrell, Texas, tornado of 27 May 1997). Tornado HR contains winds reduced by 15% to account for reduced winds at 10 m AGL in moderately rough terrain. Tornado SM represents a more frequently observed class of moderately intense, but small, tornadoes (Wurman et al. 1996; Wurman and Gill 2000).

While the actual MH and BC tornadoes passed over mostly rural or low-population-density suburban regions (Fig. 2), the paths of the simulated tornadoes are chosen so as to cross densely populated urban residential areas and the downtown of Chicago, Illinois (Fig. 9). The higher population density of Chicago compared to Oklahoma City is striking. Thirty-five-kilometer-long southwest to northeast tracks, typical of many long-track tornadoes (Grazulis 1993; Speheger et al. 2002; Brooks 2004), are overlaid on U.S. census block data regions. The number of



FIG. 7. Terrain and foliage near the site of the in situ tornado wind observation on FM 1228 near Jayton, TX. The terrain was very flat and low scrub trees dominated. Trees extending above 10 m AGL can be seen in the background of the top photograph.

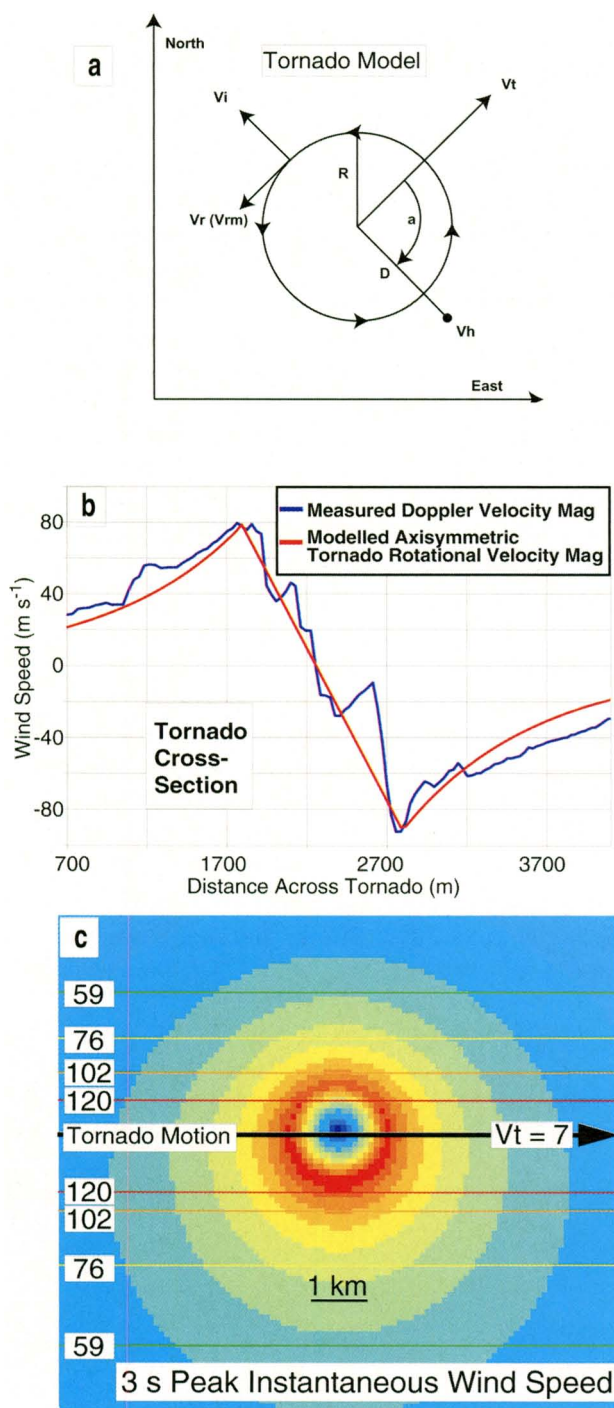


FIG. 8. Model wind field structure. (a) Schematic of model wind field. (b) Cross section of Doppler velocity across actual and model tornado. An azimuthal cross section through the Mulhall tornado shows the actual Doppler velocities (blue) measured in the core flow and nearby regions and the model's axisymmetric rotational velocity (red). (c) Top-down view of instantaneous wind speed in simulated tornado and $|V_h|$ wind swaths (m s^{-1}). The swath of peak $|V_h|$ is displaced south of the track of the tornado center due to the additive nature of V_h and V_t on this side of the tornado.

housing units and population impacted by different thresholds of peak $|V_h|$ (43, 59, 76, 102, and 120 m s^{-1}) are calculated using ArcMap 9.1 software and the tornado model (Fig. 10). To account for census blocks that are only partially covered by the wind swaths, the totals are adjusted by half of the difference between the value if all and the value if none of the partially impacted blocks are counted. This adjustment involves only about 10% of the blocks covered by the widest wind swaths, but all impacted blocks in the narrowest swaths. The areal coverage of high $|V_h|$ and the number of residents and housing units impacted are shown in Tables 2 and 3.

No attempt is made here to correct for differences in terrain or surface roughness between the environments of the observed tornadoes used to constrain the stimulations (i.e., BC, MH, and others) and the urban areas over which the simulated tornadoes cross. It is possible that surface roughness in highly built-up urban areas would be higher, reducing near-surface winds. It is also possible that local enhancements of winds could occur. However, the bulk of the tracks of the simulated tornadoes are over regions in which two- and three-story low-rise residential structures predominate, so the differences between the environments of the observed and simulated tornadoes may not be significant.

To calculate the extent of damage to impacted structures, tables correlating the degree of damage (DOD) to peak $|V_h|$ from the Enhanced Fujita Scale (EF-Scale) (Marshall 2004; as updated by J. McDonald 2006, personal communication) are used. Accordingly, one- and two-family residential structures exposed to $|V_h| > 76 \text{ m s}^{-1}$ are completely destroyed, while those exposed to $|V_h|$ of $59\text{--}76 \text{ m s}^{-1}$ experience collapse of exterior walls and roofs. Three-story residential structures suffer collapse of the top two floors at $|V_h| > 76 \text{ m s}^{-1}$. Satellite imagery is used to determine that the majority of housing units in the affected areas are of these two types (Fig. 11). According to the EF-Scale, tall apartment and office buildings on the Chicago shoreline and in the downtown area are more resistant to extreme winds and would not suffer "permanent structural damage" unless $|V_h| > 102 \text{ m s}^{-1}$, so the calculations for these areas are conducted separately (Table 3). No attempt is made here to account for the feedback effect of debris loading on the tornado wind speed structure itself (Lewellen et al. 2004) or on the damage-enhancing effects of excessive debris loading on buildings.

There are no studies that relate the probability of death for residents to the DOD in these structures. However, it is likely that the risk of death is high if

one is inside a single-family house that is totally destroyed (Fig. 12), with no walls standing (DOD: 9 or 10 @ $|V_h| > 76 \text{ m s}^{-1}$ wind speed), or in the collapsed upper two floors of a three-story apartment (DOD: 10 @ $|V_h| > 80 \text{ m s}^{-1}$). Warning times for tornadoes, in stark contrast to those for hurricanes, are typically only 10 minutes (Simmons and Sutter 2005), often providing inadequate time for evacuation. The probability of dying in the actual BC tornado ranged from 1% to 3% in the regions that experienced F4 and F5 damage [based on the location of fatalities from D. A. Speheger (2006, personal communication) and the F4/F5 maps from Speheger et al. (2002)]. However, the tornado formed well to the southwest of Oklahoma City and residents had unusually long warning times. Additionally, it is likely that residents of Oklahoma City are more aware of tornado hazards and likely to respond to warnings more efficiently than residents of many other cities, including Chicago. In the Spencer, South Dakota, tornado (Wurman and Alexander 2005), the destruction of fewer than 30 structures at the F3 or F4 level resulted in six deaths, representing a much higher

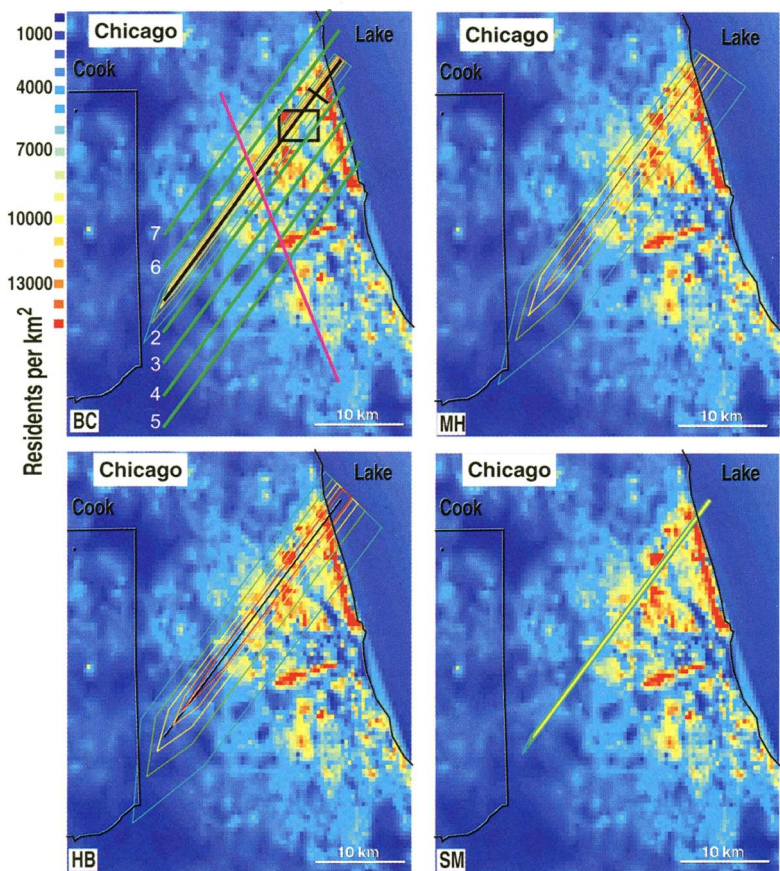


FIG. 9 (TOP RIGHT). Tracks of simulated tornadoes across Chicago. Track of the tornado center (black) and outlines of regions impacted by 120 (red), 102 (orange), 76 (yellow), 59 (green), and 43 m s^{-1} (cyan) peak wind speeds shown. Population densities are much higher than those in Oklahoma City, over which the intense BC tornado actually crossed (see Fig. 2) Black rectangle is region illustrated in Fig. 10. Black cross-track line (BC panel) is break between low-rise housing and high-rise housing areas; green alternate tornado center tracks (BC panel) are those used in sensitivity study. Pink track is “worst case” track (HN in Table 2) through length of high-density residential regions.

FIG. 10 (RIGHT). Tornado peak wind swath detail. Regions enclosed by winds of 43, 59, 76, 102, and 120 m s^{-1} are shown for tornadoes BC and HB. U.S. census block polygons fully interior to the 76 m s^{-1} peak 3-s-duration wind contour, corresponding to DOD:9 for single- and dual-family residences, are highlighted with black boundaries. The population residing within each polygon is shaded. Pink rectangles labeled “x,” “y,” and “z” are satellite photo insets (Fig. 11).

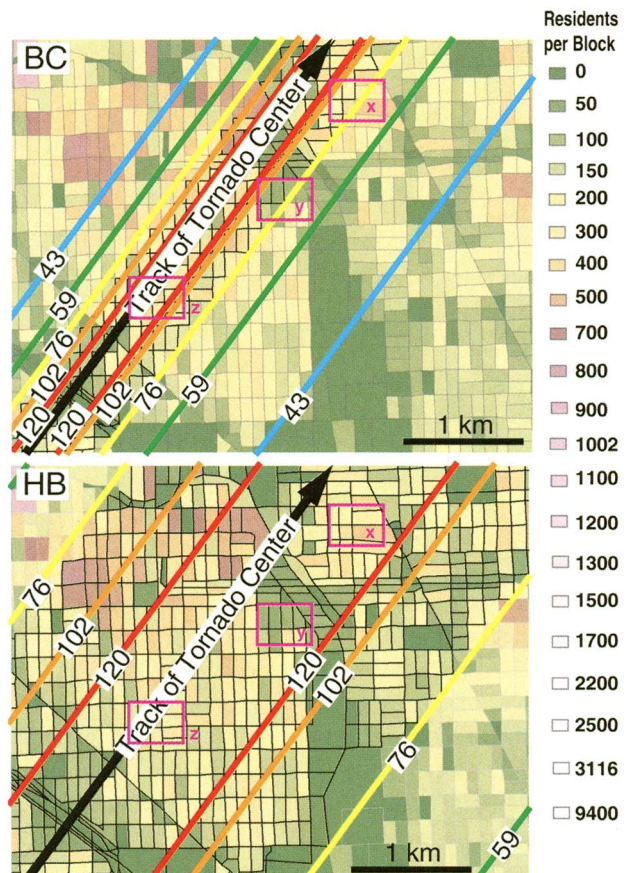


TABLE 2. Impacts of tornadoes over low-rise residential areas of Chicago. Area enclosed by various $|V_h|$ thresholds, number of residents impacted, number of housing units impacted and DOD, and deaths listed.

Area (km ²)						Residents (1000)					Housing Units impacted (1000) and deaths					
$ V_h $	43	59	76	102	120	43	59	76	102	120	43	59	76	102	120	Deaths (1000s)
EF-Scale DOD (single- and dual-family residences/three-story apartments)											4/2	7/4	9/5	10/6	10/6	
MH	221	106	61	18	—	1,005	532	328	104	—	337	182	111	36	—	33
BC	71	38	23	14	8	359	197	126	75	47	124	67	43	25	16	13
HB	275	143	84	45	26	1,141	699	446	262	169	404	239	152	88	28	45
HR	204	106	63	27	—	892	530	337	154	—	306	181	115	53	—	34
SM	17	10	3	—	—	96	54	29	—	—	34	19	10	—	—	3
HN	275	143	84	45	26	1,699	1,009	630	363	222	530	300	185	106	65	63
H2	(similar to HB, not calculated)					1,011	601	398	248	163	340	195	128	79	51	40
H3	(similar to HB, not calculated)					926	540	348	203	134	298	175	75	62	41	35
H4	(similar to HB, not calculated)					904	514	323	184	120	293	167	107	64	42	32
H5	(similar to HB, not calculated)					908	503	317	214	143	304	168	101	69	45	32
H6	(similar to HB, not calculated)					1,055	585	350	199	129	366	202	120	69	45	35
H7	(similar to HB, not calculated)					1,023	511	275	149	86	361	181	98	53	31	28

TABLE 3. Impacts of tornadoes over high-rise apartment and office areas of Chicago. Area enclosed by various $|V_h|$ thresholds (m s⁻¹), number of residents impacted, number of housing units impacted and DOD, and deaths listed.

Area (km ²)						Residents (1000)					Housing Units impacted (1000) and deaths					
$ V_h $	43	59	76	102	120	43	59	76	102	120	43	59	76	102	120	Deaths
EF-Scale DOD (> 20 story high-rise buildings)											3	6	9	10	10	
MH	24	16	11	3	—	261	172	110	28	—	115	74	45	12	—	280
BC	6	4	2	1	1	79	45	30	19	13	33	18	12	8	5	190
HB	34	22	15	9	6	310	230	154	91	59	136	97	63	36	24	910
HR	27	17	11	5	—	274	178	119	48	—	117	75	48	20	—	480
SM	0.5	0.3	0.1	—	—	8	5	3	—	—	4	2	1	—	—	—
HN	(does not pass through high-rise lakefront or downtown region)															
H2	(similar to HB, not calculated)					452	276	179	116	78	210	127	84	56	39	1160
H3	(similar to HB, not calculated)					402	260	165	101	67	207	137	85	50	33	1010
H4	(similar to HB, not calculated)					305	192	139	89	60	172	108	81	52	35	890
H5	(similar to HB, not calculated)					208	147	95	58	34	125	90	57	34	21	580
H6	(similar to HB, not calculated)					325	208	147	91	62	135	80	56	34	23	910
H7	(similar to HB, not calculated)					202	118	72	43	28	82	44	28	17	11	430

average death rate per destroyed structure, 20%, and per resident in the F3/F4 swath, about 6%. However, all of these deaths occurred in a single structure, housing the elderly. The probability of dying in a tornado is likely sensitive to the time of day, the day of week, and the meteorological conditions, since these determine whether people are in their homes, driving, whether they are asleep or awake, and whether the tornado would be visible or surrounded by rain, and, as in Spencer, the age and health of the residents, with the very elderly and very young being particularly vulner-

able to injury and slower to evacuate to safe locations. The Spencer tornado family formed well to the west of Spencer, 34 minutes before the town was impacted (Alexander and Wurman 2005). The formal warning lead time in Spencer was only six minutes (USDOC 1998), which is less than average, but some residents were aware of tornado warnings and the existence of tornadoes to the west of the town. We estimate, *crudely*, that the probability of death to residents is typically 10% in totally destroyed structures if there is little warning time. While lower peak wind speeds



FIG. 11. Aerial photographs of densely populated regions of Chicago, insets “x,” “y,” and “z” in Fig. 10, containing mainly low-rise residential structures. Housing units are packed densely on small lots. A mixture of three-story apartments and single-family units is typical across a wide region of the Chicago metropolitan area, as well as other cities dominated by older construction such as New York City. (lower right) Aerial photograph of medium-density-populated region of Moore, OK, containing mainly low-rise residential structures, revealing that the less dense packing of housing units typical in the Oklahoma City metropolitan area and other cities are dominated by newer construction and larger residential lots.

FIG. 12. Destroyed homes in Spencer, SD, May 1998. Winds at 30 m AGL in the tornado were measured by a DOW radar. Using these data, and the axisymmetric model, ground-relative 3-s-duration winds of $80\text{--}90\text{ m s}^{-1}$ were calculated to have occurred in the foreground region in this photograph, near the intersection of 4th and Wilcox Streets. These DOW-based wind speeds are consistent with the EF-Scale wind speeds, $> 76\text{ m s}^{-1}$, expected for the observed DOD:9.



still cause substantial damage to homes—that is, $|\mathbf{V}_h| > 59 \text{ m s}^{-1}$ causes DOD:5 to single-family homes, with top-floor exterior walls collapsed and large sections of roof removed—it is likely that the risk of death

in partially damaged homes is much less. In our calculations, we assume zero deaths in these structures. The risks in high-rise apartment buildings are less clear and there is scant historical basis for making estimates. The

highest EF-Scale DOD:6 is described as “permanent structural damage,” which occurs with $|\mathbf{V}_h| > 102 \text{ m s}^{-1}$. We assume that the probability of death in such structures is only 1%. The actual probability of dying could exceed these crude estimates. Nevertheless, the number of people living in the affected structures is quite large, resulting in estimated deaths as shown in Tables 2 and 3. Most deaths occur in the smaller residential structures. In the simulations over the Chicago metropolitan area, the large and/or intense tornadoes kill 13,000–45,000 people. Even the smaller, moderate-intensity tornado kills about 3,000 as $|\mathbf{V}_h| > 76 \text{ m s}^{-1}$ impacts 29,000 housing units. *It is important to note that a lower, but still plausible, assumed death rate in low-rise residential structures, say only 1% due to a long lead-time warning or other factors, would result in many fewer deaths.*

The financial costs would be correspondingly high. The value of the destroyed homes and property are difficult to estimate precisely. However, the 239,000 low-rise housing units substantially damaged by $|\mathbf{V}_h| > 59 \text{ m s}^{-1}$ in tornado HB, even if valued at only \$100,000 each, would require \$23.9 billion to replace. Depending on the precise track of the tornado, $|\mathbf{V}_h| > 102 \text{ m s}^{-1}$, extending over a 1,985-m-wide swath covering several square kilometers of the downtown area, would cause “permanent structural damage” to dozens to hundreds of high-rise offices and apartments. Such structures can cost over \$200 million to replace, not including the contents or the cost of lost business activities. It is likely that “permanent structural damage” to 100 such structures would add another \$20 billion to the cost of the tornado.

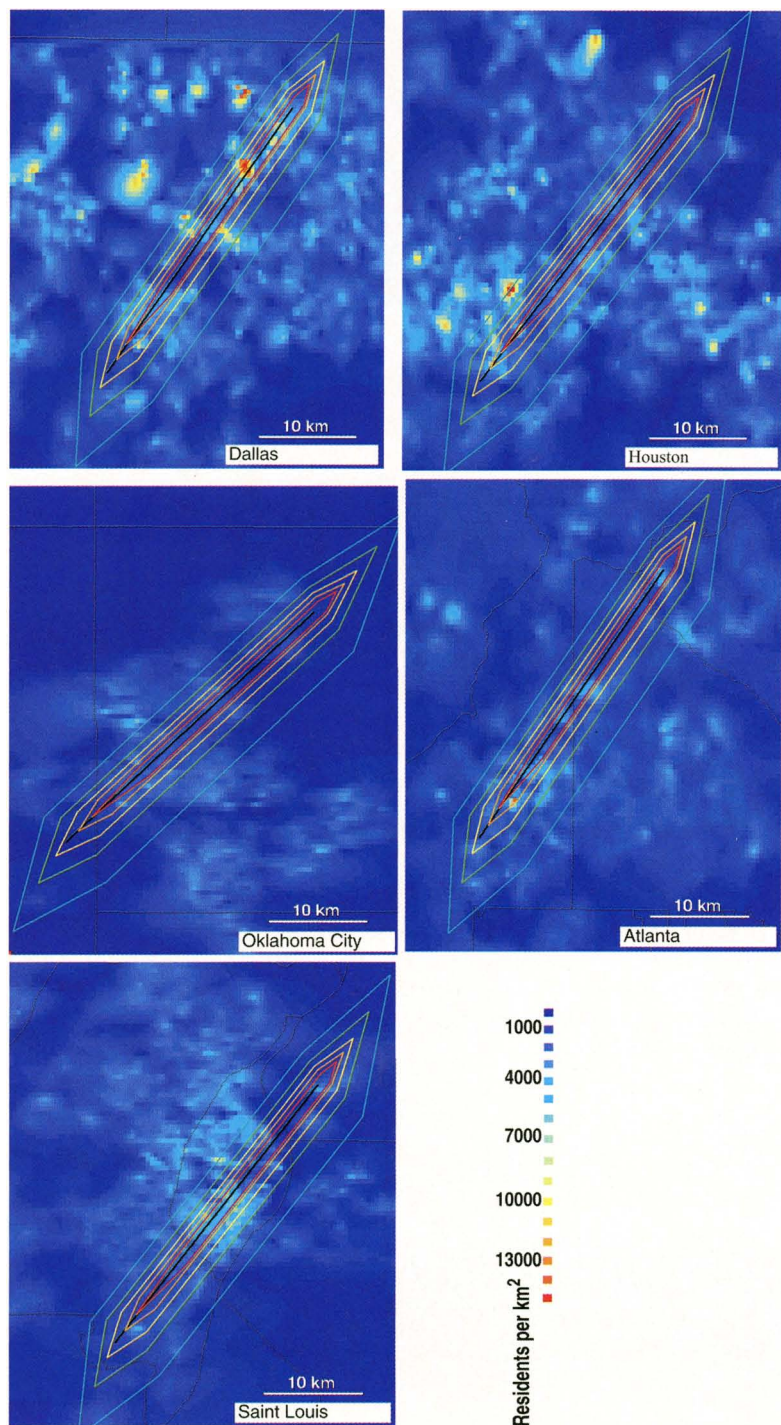


FIG. 13. Tracks and wind swaths of simulated tornado HB across several different metropolitan regions. Population density is shaded. Population density and the resultant potential impacts from tornadoes vary greatly from older cities such as Chicago to newer cities such as Oklahoma City and Dallas.

TABLE 4. Impacts of tornadoes crossing different metropolitan areas. Number of residents (in thousands) impacted by $|\mathbf{V}_h| > 76 \text{ m s}^{-1}$ in Chicago (CHI), New York City (NYC), the District of Columbia (DC), Saint Louis (STL), Dallas–Fort Worth (DAL), Houston (HOU), Atlanta (ATL), and Oklahoma City (OKC). Chicago is repeated for comparison purposes. The majority of residents in the impacted regions live in low-rise single-family dwellings, but not all. Deaths are crudely estimated at 10% of those impacted by $> 76 \text{ m s}^{-1}$ winds, so, e.g., the 438,000 residents exposed to $> 76 \text{ m s}^{-1}$ winds by the MH tornado in Chicago results in 43,800 estimated deaths.

	CHI	NYC	DC	STL	DAL	HOU	ATL	OKC
MH	438			143	221	170	149	83
BC	157	192	65	50	80	67	55	33
HB	600			199	297	237	195	112
HR	456			147	233	174	153	87
SM	32	44	19	16	29	20	20	11

Sensitivity of impacts to particular track. The sensitivity of these results to the exact choice of tornado track is explored by repeating the above calculations for tracks that begin at several different latitudes at 3-km intervals (Fig. 9; Tables 2 and 3). While tracks that cover proportionately more rural and less dense suburban regions impact fewer people, the number of destroyed structures and impacted residents of the alternate tornadoes are almost always greater than 50% of that of the base-track tornado (note that results from simulations of alternate tracks of tornado structure HB are the only ones listed in Tables 2 and 3). A more unusual, but potentially worse, tornado track, crossing from north-northwest to south-southeast across Chicago (possible in a northwest flow regime) (Fig. 9; Tables 2 and 3), results in 630,000 residents in 185,000 housing units being impacted by $|\mathbf{V}_h| > 76 \text{ m s}^{-1}$ and 363,000 residents in 106,000 housing units by $|\mathbf{V}_h| > 102 \text{ m s}^{-1}$, resulting in 63,000 deaths. Some tracks that impact fewer single-family residential structures, resulting in fewer deaths, pass directly over the Chicago downtown and lakefront, destroying proportionally more high-value, high-rise office buildings.

Tornado impacts in other major cities. Other major cities are vulnerable to the impact of violent tornadoes. Several cities in the Midwestern and southern United States exist in regions that frequently experience tornadoes, including Oklahoma City, Saint Louis, Missouri, Dallas–Fort Worth and Houston, Texas, and Atlanta, Georgia (Grazulis 1993). Violent tornadoes have occurred near the District of Columbia (Manning and Zubrick 2004) and New York City (Grazulis 1993). While the precise conditions that lead to violent tornadoes are not known, the historical record suggests that large, violent tornadoes are much less likely east of the Appalachian Mountains. The effects of the various tornadoes crossing several

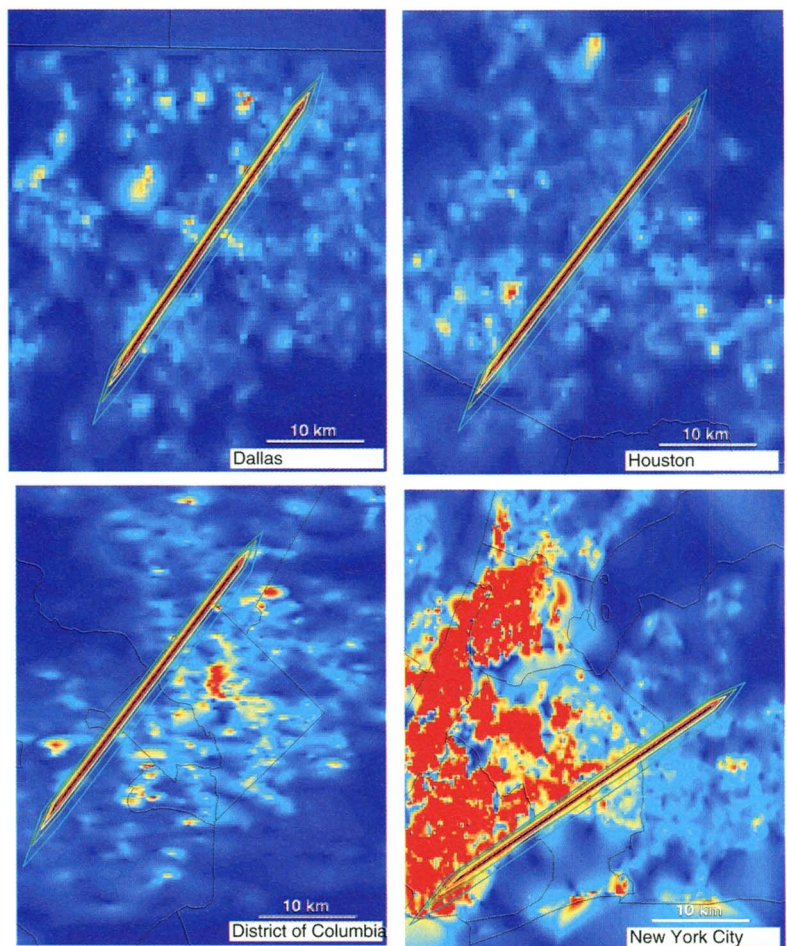
metropolitan areas are calculated, except that the calculation excludes unlikely large, violent tornadoes for New York City and the District of Columbia. The major factor determining the level of impact is the population density in the low-rise residential regions over which the tornadoes track (Figs. 13 and 14). Cities containing large regions with new lower-density residential construction, including Oklahoma City, experience lesser impacts. However, the impact of long-track violent tornadoes in older cities, particularly from tornadoes crossing suburban New York City, would be even larger than that experienced if the corresponding tornadoes crossed Chicago (Table 4). The economic cost of the effects of $|\mathbf{V}_h| > 102 \text{ m s}^{-1}$ resulting in “permanent structural damage” to thousands of high-rise structures in Manhattan would far exceed the economic cost of the destruction of several such structures on 11 September 2001, though the number of fatalities is difficult to estimate. The impacts in Houston, Atlanta, Saint Louis, and the District of Columbia are less than that in New York City or Chicago, but are still extremely high.

The simulated BC tornado crossing the most densely populated portions of the Oklahoma City metropolitan area (recall that the actual BC tornado crossed over only limited regions of moderately dense development) results in 33,000 people being impacted by $|\mathbf{V}_h| > 76 \text{ m s}^{-1}$. Assuming a 10% probability of death, where $|\mathbf{V}_h| > 76 \text{ m s}^{-1}$, the estimated death toll is 3,300, compared to the 36 people who actually died in the tornado that crossed Oklahoma City on 3 May 1999. This discrepancy likely exists because the simulated BC passed through a greater length of high-density, low-rise residential neighborhoods compared to the 3 May 1999 tornado, because the actual tornado narrowed considerably before crossing Moore, and because the probability of dying in the actual tornado was between 1% and 3% in neighbor-

FIG. 14 (THIS PAGE AND NEXT). Tracks and wind swaths of simulated tornado BC across several different metropolitan regions. Otherwise, same as in Fig. 13.

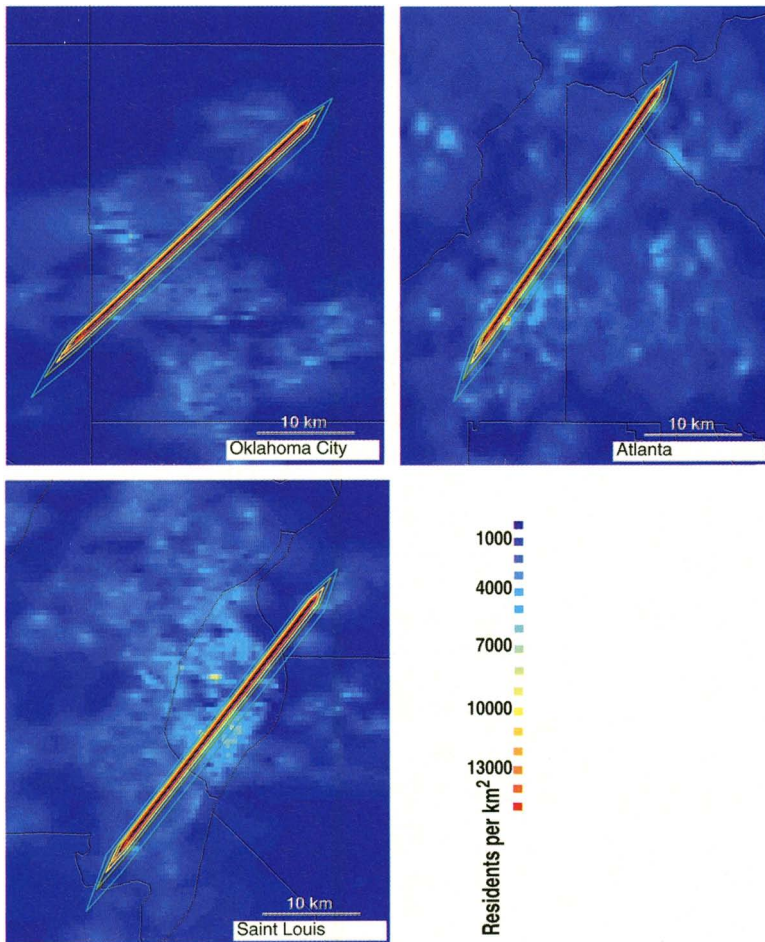
hoods affected by F4 and F5 damage, possibly due to unusually long warning lead times.

CONCLUSIONS. Simulated tornadoes with wind field structures similar to those observed, and potentially worse plausible tornadoes, crossing a densely populated urban region such as Chicago, could cause widespread damage and loss of life on a scale that has not been observed historically with tornadoes. Despite the small size of tornadoes, they occur with little warning and because of their intensity they can cause nearly total destruction of many inhabited structures, resulting in potentially high death rates. The largest and most intense tornadoes could completely destroy structures across more than 90 km², killing perhaps 10% of the residents in these structures, resulting in as many as 13,000–45,000 deaths in densely populated cities such as Chicago. If, due to better warnings, efficient public response, or better shelters, the death rate in destroyed structures were only 1%, substantial death tolls of 1,300–4,500 might still be expected. These are comparable to or exceed the tolls from historical hurricanes such as those that impacted Galveston, Texas, in 1900, causing 8,000 deaths, or New Orleans, Louisiana, in 2005, causing over 1,300 deaths. The scale of potential damage is far larger than that of the San Francisco, California, earthquake of 1906, which killed 700 people and destroyed buildings over a 13 km² area. The cost of replacing tornado-destroyed structures could exceed \$40 billion. This total is less than the cost of damaged infrastructure from Hurricane Katrina (2005), due to the much smaller area of damage, but is higher than that in Hurricane Andrew (1992) (Bryant 1991; Robinson 1993; NHC 2005). Worst-case, but less likely, scenarios where tornadoes move lengthwise along the highest-density, low-rise residential areas, along the lakefront of Chicago, or with curved tracks, could result in even higher damage



and death tolls. Severe tornado impacts are possible in other Midwestern and southern cities such as Dallas, Oklahoma City, Saint Louis, Atlanta, and Houston. Though it is unlikely that the largest and most intense tornadoes would impact eastern cities such as New York City or the District of Columbia, violent tornadoes could still result in widespread structural damage and high death tolls exceeding 1,000–10,000, depending on the death rate in destroyed structures.

We recommend that awareness of the potentially catastrophic impacts of tornadoes in major urban areas be raised and that emergency managers have contingency plans for these rare, but possible, events. The eventuality of intense tornadoes crossing urban areas cannot be avoided. However, longer warning lead times and improved credibility of the warnings resulting from an increased understanding of the mechanisms of violent tornadoogenesis and better observations of thunderstorms capable of producing violent tornadoes would enable the public in densely populated regions more time to seek robust shelter, thereby reducing the



death rates associated with destroyed structures. In addition, we hope that an increased awareness by emergency managers and the public concerning the damage and fatality potential of intense tornadoes in urban areas will increase the speed and efficiency with which the urban public is able to seek robust shelter from violent tornadoes.

ACKNOWLEDGEMENTS. Supported in part by National Science Foundation Grants NSF-ATM-0437505, NSF-ATM-0437512, and NSF-ATM-0437898. Doug Speheger provided track and fatality data for the 3 May 1999 tornadoes. The DOWs have received support from the National Center for Atmospheric Research. Herb Stein, David Dowell, William Martin, Jeff Beck, and Justin Walker helped the authors collect the data presented here.

REFERENCES

Alexander, C., and J. Wurman, 2005: The 30 May 1998 Spencer, South Dakota, storm. Part I: The structural evolution and environment of the tornadoes. *Mon. Wea. Rev.*, **133**, 72–96.

Bluestein, H. B., and A. L. Pazmany, 2000: Observations of tornadoes and other convective phenomena with a mobile, 3-mm wavelength, Doppler radar: The spring 1999 field experiment. *Bull. Amer. Meteor. Soc.*, **81**, 2939–2951.

—, W.-C. Lee, M. Bell, C. C. Weiss, and A. L. Pazmany, 2003: Mobile Doppler radar observations of a tornado in a supercell near Bassett, Nebraska, on 5 June 1999. Part II: Tornado-vortex structure. *Mon. Wea. Rev.*, **131**, 2968–2984.

—, C. C. Weiss, and A. L. Pazmany, 2004: The vertical structure of a tornado near Happy, Texas, on 5 May 2002: High-resolution, mobile, W-band, Doppler radar observations. *Mon. Wea. Rev.*, **132**, 2325–2337.

Brooks, H. E., 2004: On the relationship of tornado path length and width to intensity. *Wea. Forecasting*, **19**, 310–319.

—, and C. A. Doswell III, 2001: Normalized damage from major tornadoes in the United States: 1890–1999. *Wea. Forecasting*, **16**, 168–176.

Bryant, E. A., 1991: *Natural Hazards*. Cambridge University Press, 294 pp.

Burgess, D. W., M. A. Magsig, J. Wurman, D. C. Dowell, and Y. Richardson, 2002: Radar observations of the 3 May 1999 Oklahoma City tornado. *Wea. Forecasting*, **17**, 456–471.

Doswell, C. A., III, and D. Burgess, 1988: On some issues of United States tornado climatology. *Mon. Wea. Rev.*, **116**, 495–501.

—, R. Edwards, R. L. Thompson, J. A. Hart, and K. C. Crosbie, 2006: A simple and flexible method for ranking severe weather events. *Wea. Forecasting*, **21**, 939–951.

Doviak, R. J., and D. S. Zrnic, 1993: *Doppler Radar and Weather Observations*. Academic Press, 562 pp.

Dowell, D. C., C. Alexander, J. Wurman, and L. Wicker, 2005: Centrifuging of hydrometers and debris in tornadoes: Radar reflectivity patterns and wind-measurement errors. *Mon. Wea. Rev.*, **133**, 1501–1524.

Fiedler, B. H., and R. Rotunno, 1986: A theory for the maximum windspeeds in tornado-like vortices. *J. Atmos. Sci.*, **43**, 2328–2340.

Forbes, G., 2006: Meteorological aspects of high-impact tornado outbreaks. *Extended Abstracts, Symp. on the*

- Challenges of Severe Convective Storms*, Atlanta, GA, Amer. Meteor. Soc., CD-ROM, P1.12.
- Fujita, T. T., 1971: Proposed characterization of tornadoes and hurricanes by area and intensity. SMRP Research Rep. 91, University of Chicago, 15 pp.
- , 1992: *Mystery of Severe Storms*. The University of Chicago Press, 298 pp.
- Glenday, C., 2005: *Guinness Book of World Records 2007*. Guinness Ltd., 288 pp.
- Grazulis, T. P., 1993: *Significant Tornadoes: 1680–1991*. Environmental Films, 1326 pp.
- Lee, J., T. Samaras, and C. Young, 2004: Pressure measurements at the ground in an F4 tornado. Preprints, *22d Conf. on Severe Local Storms*, Hyannis, MA, Amer. Meteor. Soc., CD-ROM, 15.4.
- Lee, W. C., and J. Wurman, 2005: Diagnosed three-dimensional axisymmetric structure of the Mulhall tornado on 3 May 1999. *J. Atmos. Sci.*, **62**, 2373–2393.
- Letzmann, J., 1923: Das Bewegungsfeld im Fuss einer fortschreitenden Wind- oder Wasserhose (The flow field at the base of a progressing tornado). Ph.D. thesis, University of Dorpat, 80 pp. [Available online at www.essl.org/pdf/Letzmann1923/Letzmann1923.pdf.]
- Lewellen, D. C., B. Gong, and W. S. Lewellen, 2004: Effects of debris on near-surface tornado dynamics. Preprints, *22d Conf. on Severe Local Storms*, Hyannis, MA, Amer. Meteor. Soc., CD-ROM, 15.5.
- Lewellen, W. S., D. C. Lewellen, and R. I. Sykes, 1997: Large-eddy simulation of a tornado's interaction with the surface. *J. Atmos. Sci.*, **54**, 581–605.
- Manning, D. R., and S. M. Zubrick, 2004: Doppler radar analysis of the 28 April 2002 La Plata, MD tornadic supercell. *22d Conf. on Severe Local Storms*, Hyannis, MA, Amer. Meteor. Soc., CD-ROM, 13.5.
- Marshall, T. P., 2004: The enhanced Fujita (EF) scale. Preprints, *22d Conf. on Severe Local Storms*, Hyannis, MA, Amer. Meteor. Soc., CD-ROM, 3B.2.
- McCarthy, D., and J. Schaefer, 2005: 2004 year in tornadoes: What a year it was! Preprints, *34th Conf. on Broadcast Meteorology*, Washington, DC, Amer. Meteor. Soc., CD-ROM, 2.1.
- NHC, cited 2005: Tropical Storm Katrina. [Available online at www.nhc.noaa.gov/2005atlan.shtml or www.nhc.noaa.gov/pdf/TCR-AL122005_Katrina.pdf.]
- Phan, L. T., and E. Simiu, 1998: The Fujita tornado intensity scale: A critique based on observations of the Jarrell tornado of May 27, 1997. NIST Tech. Note 1426, 20 pp.
- Rae, S., and J. Stefkovich, 2000: The tornado damage risk assessment predicting the impact of a big outbreak in Dallas-Fort Worth, Texas. *Extended Abstracts*, *20th Conf. on Severe Local Storms*, Orlando, FL, Amer. Meteor. Soc., 295–296.
- Robinson, A., 1993: *Earth Shock: Hurricanes, Volcanoes, Earthquakes, Tornadoes and Other Forces of Nature*. Thames and Hudson, 304 pp.
- Simmons, K. M., and D. Sutter, 2005: WSR-88D radar, tornado warnings, and tornado casualties. *Wea. Forecasting*, **20**, 301–310.
- Speheger, D. A., C. A. Doswell, and G. J. Stumpf, 2002: The tornadoes of 3 May 1999: Event verification in central Oklahoma and related issues. *Wea. Forecasting*, **17**, 362–381.
- USDOC, 1998: Service assessment: Spencer, South Dakota, tornado May 30, 1998. NOAA/NWS, 18 pp.
- Winn, W. P., S. J. Hunyady, and G. D. Aulich, 1999: Pressure at the ground in a large tornado. *J. Geophys. Res.*, **104D**, 22 067–22 082.
- World Meteorological Organization, 2004: Technical regulations, Vol. II, Meteorological Service for International Air Navigation, WMO-No. 49. [Available from WMO 41 Giuseppe-Mota, Case postale no. 2300, CH-1211 Geneve 2, Geneva, Switzerland.]
- Wurman, J., 2001: The DOW mobile multiple Doppler network. Preprints, *30th Int. Conf. on Radar Meteorology*, Munich, Germany, Amer. Meteor. Soc., 95–97.
- , 2002: The multiple-vortex structure of a tornado. *Wea. Forecasting*, **17**, 473–505.
- , and S. Gill, 2000: Finescale radar observations of the Dimmitt, Texas (2 June 1995), tornado. *Mon. Wea. Rev.*, **128**, 2135–2164.
- , and T. Samaras, 2004: Comparison of in-situ and DOW Doppler winds in a tornado and RHI vertical slices through 4 tornadoes during 1996–2004. Preprints, *22d Conf. on Severe Local Storms*, Hyannis, MA, Amer. Meteor. Soc., CD-ROM, 15.4.
- , and C. Alexander, 2005: The 30 May 1998 Spencer, South Dakota, storm. Part II: Comparison of observed damage and radar-derived winds in the tornadoes. *Mon. Wea. Rev.*, **133**, 97–119.
- , J. Straka, and E. Rasmussen, 1996: Fine scale Doppler radar observation of tornadoes, *Science*, **272**, 1774–1777.
- , —, —, M. Randall, and A. Zahrai, 1997: Design and deployment of a portable, pencil-beam, pulsed, 3-cm Doppler radar. *J. Atmos. Oceanic Technol.*, **14**, 1502–1512.
- , Y. Richardson, C. Alexander, S. Weygandt, and P.-F. Zhang, 2007a: Dual-Doppler and single-Doppler analysis of a tornadic storm undergoing mergers and repeated tornadogenesis, *Mon. Wea. Rev.*, in press.
- , —, —, —, and —, 2007b: Dual-Doppler analysis of winds and vorticity budget terms near a tornado. *Mon. Wea. Rev.*, in press.